Science of the Total Environment 654 (2019) 933–941

Contents lists available at ScienceDirect

Science of the Total Environment

journal homepage: www.elsevier.com/locate/scitotenv

Quick start-up and stable operation of a one-stage deammonification reactor with a low quantity of AOB and ANAMMOX biomass

Yifeng Yang [a,b], Yuan Li [b,c], Zaoli Gu [a,b], Feng Lu [a], Siqing Xia [a,*], Slawomir Hermanowicz [b,c]

[a] State Key Laboratory of Pollution Control and Resource Reuse, College of Environmental Science and Engineering, Tongji University, 1239 Siping Road, Shanghai 200092, PR China
[b] Department of Civil and Environmental Engineering, University of California, Berkeley, CA 94720, USA
[c] Tsinghua-Berkeley Shenzhen Institute, Tsinghua University Shenzhen, PR China

HIGHLIGHTS

- A novel single-stage deammonification system by immobilized AOB and ANAMMOX was developed.
- The start-up time of deammonification could be shortened to 10 days with only 0.4 g-VSS L^{-1} biomass.
- The micro-profiles of DO and pH in gel layers confirmed excellent spatial gel structure.
- The microbial community distribution studied by FISH analysis was corresponded to the micro-profiles of DO and pH.

GRAPHICAL ABSTRACT

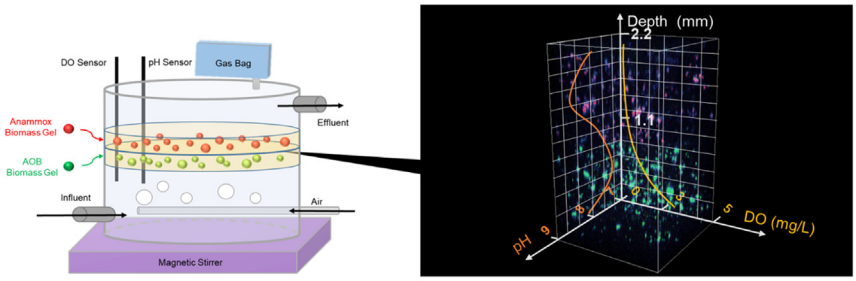

Schematic of immobilized AOB and ANAMMOX bacteria reactor (IAAR)

In Situ FISH Analysis of the AOB and ANAMMOX with pH and DO concentration profiles

ARTICLE INFO

Article history:
Received 4 September 2018
Received in revised form 4 November 2018
Accepted 5 November 2018
Available online 06 November 2018

Editor: Zhen (Jason) He

Keywords:
Start-up of deammonification
Gel immobilization
ANAMMOX
Nitritation
Ammonium wastewater treatment

ABSTRACT

In this study, a quick start-up of one-stage deammonification in an immobilized aerobic ammonium oxidizing bacteria (AOB) and anoxic ammonium oxidizing (ANAMMOX) bacteria up-flow reactor (IAAR) was successfully achieved. With the aid of gel layers, AOB and ANAMMOX bacteria had excellent spatial distribution, theoretically meeting dissolved oxygen requirements for the simultaneous processes of aerobic and anaerobic ammonium oxidizing. The results indicated that an IAAR containing 0.4 g-VSS L^{-1} immobilized biomass achieved a nitrogen removal rate (NRR) of 0.53 kg-N m^{-3} d^{-1} after only 10 days of operation and subsequently reached a maximum nitrogen removal rate (NRR_{max}) of 3.73 kg-N m^{-3} d^{-1}. The micro-profiles of DO and pH were measured using microelectrodes to help understand the stratification of the microbial processes inside the gel layers. The distribution of AOB and ANAMMOX bacteria within the gel layers was verified using fluorescence in situ hybridization (FISH) analysis. The community distribution in the FISH three-dimensional images closely corresponded to the micro-profiles of DO concentration and pH, enabling rapid adaptation and stable operation of the reactor seeded with a quite low quantity of biomass.

1. Introduction

Nitrogen is among the major sources of pollution in water bodies. Fixed nitrogen such as ammonium, nitrite, and nitrate must be removed to avoid eutrophication and the high frequency of algal blooms in the environment. The treatment methods of wastewater containing nitrogen included physical, chemical, and biological processes. Although chemical treatment such as advanced oxidation processes are considered highly effective, the operational expense is high (Cai et al., 2018; Luo et al., 2018; Min et al., 2018; Xiao et al., 2018; Yang et al., 2017). The most widely applied method for biological ammonium removal is

* Corresponding author at: 1239 Siping Road, Shanghai 200092, PR China.
E-mail address: siqingxia@tongji.edu.cn (S. Xia).

https://doi.org/10.1016/j.scitotenv.2018.11.069
0048-9697/

a nitrification/denitrification (N/DN) system that converts ammonium into nitrogen gas. Recently, the Partial Nitrification-ANAMMOX (PN/A) process has become a subject of extensive interest because of its high efficiency and low cost in nitrogen removal (Deng et al., 2016; Jetten et al., 1998; Yan and Hu, 2009). The PN/A process is a new autotrophic nitrogen removal process with two steps: First, aerobic ammonium oxidizing bacteria (AOB) oxidize ammonium to nitrite, and second, anaerobic ammonium oxidizing (ANAMMOX) bacteria combine this nitrite with residual ammonium, forming nitrogen gas and some nitrate under a low dissolved oxygen (DO) concentration (Lackner et al., 2014). Compared to conventional nitrogen removal, the PN/A process can save up to 60% aeration energy and does not require the addition of an organic carbon source (Tokutomi et al., 2011; Van Kempen et al., 2001).

However, one-stage autotrophic deammonification has two limitations that make it difficult to use in engineering applications. First, the growth rate of ANAMMOX bacteria is very slow (Strous et al., 1998), and consequently ANAMMOX bacteria is easily washed out of the system. It is more difficult to retain a sufficient amount of ANAMMOX bacteria than AOB in a practical one-stage reactor (Strous et al., 1997). Mostly, an ANAMMOX system requires at least 90 days to complete start-up (van de Graaf et al., 1996). Second, the ANAMMOX activity is susceptible to some extraneous factors. It can be easily inhibited by low concentrations of DO and high concentrations of nitrite (Egli et al., 2001; Strous et al., 1999a). Because ammonium and nitrite as a substrate are needed for the ANAMMOX reaction, ammonium has to be partially oxidized to nitrite aerobically. When AOB and ANAMMOX bacteria grow together in one reactor, the remaining DO from the nitritation step can affect the anaerobic metabolism of the ANAMMOX bacteria. Thus, it is important to maintain the ANAMMOX bacteria and control or at least monitor the DO at low levels in the one-stage system (Corbalá-Robles et al., 2016; Gonzalez-Martinez et al., 2016; Morales et al., 2015; Xu et al., 2015).

Because of these limitations, the abilities to sustain a sufficient amount of ANAMMOX bacteria in a PN/A process reactor and to stop nitrification of nitrite are the primary focus in the development of a stable and high-efficiency autotrophic nitrogen removal system. In traditional one-stage partial nitritation-ANAMMOX reactors, such as the Complete Autotrophic Nitrogen removal Over Nitrite (CANON), Oxygen-Limited Autotrophic Nitrification/Denitrification (OLAND) and DEMON® systems, the aggregated granular sludge as the carrier of two bacteria has been proven to be successful (Gonzalez-Martinez et al., 2016; Varas et al., 2015). However, the aggregate size affects the settling properties and influences the efficiency of the microbial nitrite production and consumption. Although larger cell aggregates can be easily retained because of their own weight, both lower AOB activity and lower ANAMMOX activity have been observed with larger aggregates or sludge agglomeration (Lv et al., 2016). Currently, some researchers have immobilized AOB and ANAMMOX biomass in small gel beads. By this means, the reactor can be started and operated at high nitrogen loading rates with a low possibility of nitrite inhibition and biomass loss (Isaka et al., 2008; Isaka et al., 2013). Gel immobilization is an effective means for preventing biomass from being washed out, promoting hyper-concentrated cultures, and solving the shortage of seeding sludge (Zhu et al., 2014). Using microelectrodes, the diffusion coefficient in the naturally aggregated granular has been proven to be less than one-third of that in immobilized gel carriers (Ali et al., 2015). The engineering application of the gel immobilization process is evidenced by its current employment at 40 wastewater treatment plants (WWTPs) in Japan (Isaka et al., 2013). Although gel immobilization shows great potential in nitritation and ANAMMOX processes, the minimal biomass concentration that is necessary for successful start-up of the deammonification process has not been studied thus far.

The objective of this study was to investigate the feasibility of removing ammonia nitrogen using a very low concentration of immobilized AOB and ANAMMOX bacteria in a novel one-stage reactor. The nitritation-ANAMMOX system combined with gel immobilization similar to an artificial biofilm can be easily constructed and provides an ideal DO concentration for both bacteria at the start point, which is different from previously reported one-stage reactors. Short-term experiments were completed to evaluate the influence of the different AOB and ANAMMOX biomass concentrations on the nitrogen removal performance between the immobilized biomass and non-immobilized biomass. Then, long-term operation experiments under a different nitrogen loading rate were completed. Community distribution patterns and detailed spatial gradients of DO concentration and pH in the gel layers were obtained through two in situ analyses: microelectrode measurements and fluorescence in situ hybridization (FISH) analysis. We aimed to contribute to promoting practical application of the immobilized AOB and ANAMMOX bacteria reactor (IAAR) in wastewater treatment.

2. Materials and methods

2.1. AOB and ANAMMOX biomass

The AOB biomass for the inoculation was obtained from a lab-scale cylindrical nitritation sequencing batch reactor (Nitritation-SBR) already in operation for 11 months. The phylogenetic classification of effective bacterial sequences from the Nitritation-SBR samples at the genus level is summarized in Fig. S2, demonstrating that “Nitrosomonas” represented 23.8% of the relative abundance. The ANAMMOX biomass used for inoculation originated from a continuous anoxic ammonium oxidizing membrane reactor (ANAMMOX-MBR) reactor that had steadily worked for more than 1 year. The phylogenetic classification of the effective bacterial sequences from the samples in the ANAMMOX-MBR reactor at the genus level is summarized in Fig. S2, demonstrating “Candidatus Jettenia” represented 18.7% of the relative abundance. The enriched ANAMMOX (volatile suspended solids (VSS) at 1.1 mg L^{-1}) and AOB biomass (VSS at 2.1 mg L^{-1}) was collected and rinsed three times in a 3% phosphate-buffered saline (PBS) (pH 7.6) to remove residual substrate. Then, the sludge was centrifuged at 8000 rpm for 3 min, and the concentrated biomass was used for immobilization.

2.2. Immobilization procedure

The immobilization method included two steps as shown in Fig. 1. During the first step, ANAMMOX biomass and AOB biomass were dispersed into small floccules and diluted with the cultural medium. Equivalent volumes of 6% sodium alginate (SA) solution and two biomass concentrates were completely mixed in two beakers, respectively. During the second step, 100 mL of a mixed liquid of ANAMMOX biomass and gel was gradually poured into a rounded glass container and uniformly spread at the bottom of the container. Then, the container with the mixed liquid was filled with $CaCl_2$ solution (4%), which formed a thin gel layer 0.9–1.1 mm in thickness. The obtained solution was stored at 26 °C for 12 h for cross linking to obtain a stable SA immobilized layer in an anaerobic operating incubator. After step 1 and step 2, the first ANAMMOX gel layer was completed and rinsed three times with deionized water. The procedure of the production of the second AOB gel layer was similar to that of the ANAMMOX gel layer. The only difference was that the 12-h cross linking was completed without using an anaerobic operating incubator. The finished AOB gel layer was fixed on the upper surface of the first ANAMMOX gel layer. These two gel layers were similar to two thin pancakes clamped together, ensuring that the AOB layer has sufficient contact area to directly transfer the substrate to the ANAMMOX layer.

2.3. Reactor and experimental method

Fig. S1 shows a schematic of the IAAR for the single-stage deammonification process. The volume of the reactor was 500 mL, and the packing rate was approximately 12% (6% ANAMMOX gel and

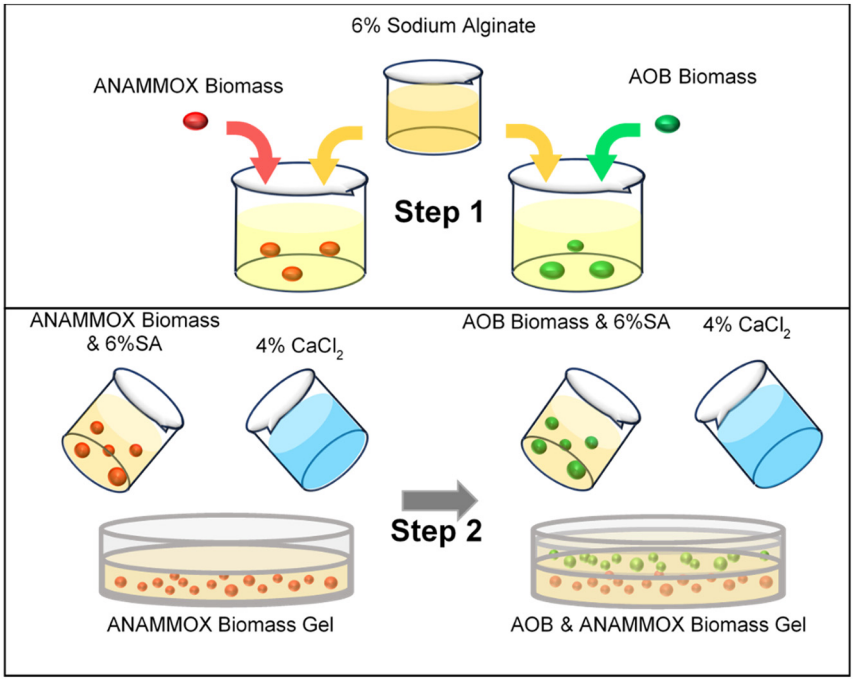

Fig. 1. Schematic of the immobilization procedure.

6% AOB gel). The reactor was provided with a thermostatic jacket and the temperature was maintained at 35 ± 1 °C. The reactor was continuously agitated at 90 rpm by a magnetic stirrer under a dark condition for 24 h. Temperature, DO, and pH sensors were installed on the lid of the IAAR for real-time monitoring. Small bubbles of air were supplied via a strip air sparger below the AOB gel layer. A CANON-MBR reactor was established to retain the suspended granular biomass by membrane, which served as a performance comparison. The volume of the CANON-MBR reactor was 500 mL, and the agitation rate and temperature were the same as those of the IAAR. The effective area of the hollow fiber membrane module was 200 cm^2 and its pore size was 0.2 μm.

The experimental design is shown in Fig. 2. Short-term and long-term tests of the IAAR were conducted in this study. Three IAARs and three CANON-MBRs were used for the short-term tests. IAAR-1, IAAR-2, and IAAR-3 were inoculated with 0.4, 0.8, and 1.2 g-VSS L^{-1} AOB and ANAMMOX biomass concentration that was immobilized in the two gel layers (see in Fig. S3). For comparison, MBR-1, MBR-2, and MBR-3 were inoculated with 0.4, 0.8, and 1.2 g-VSS L^{-1} AOB and ANAMMOX biomass concentration that was suspended granular. All the biomass for the inoculations was obtained from two cultivation reactors as previously mentioned. The concentrations of NH_4^+—N were set s 80 mg L^{-1} with a DO level of approximately 0.5 mg L^{-1} during the 7-day operation, which resulted in a nitrogen loading rate of 0.67 kg-N m^{-3} d^{-1}. The effects of the initial biomass quantity on the two types of reactors were examined. The long-term influent loading rate of the IAAR and CANON-MBR is provided in Table 1. The biomass concentrations in IAAR-L1 and IAAR-L2 were 0.4 g-VSS L^{-1} and 1.2 g-VSS L^{-1}. Meanwhile, MBR-L with a biomass concentration of 1.2 g-VSS L^{-1} was used for comparison under the same conditions. The nitrogen loading rate of IAAR increased from 0.6 to 4.1 kg-N m^{-3} d^{-1} during Phases I, II, and III. The DO concentration was maintained at a certain value of 0.5, 1, or 3 mg L^{-1} by controlling the air flow rate. The basal medium in both reactors contained 2000 mg L^{-1} of $NaHCO_3$, 27 mg L^{-1} of K_2HPO_4, 84 mg L^{-1} of $MgSO_4 \cdot 7H_2O$, 24 mg L^{-1} of $CaCl_2 \cdot 2H_2O$, 51 mg L^{-1} of NaCl, and 1 ml L^{-1} of trace element solution I and 1 ml L^{-1} of trace element solution II (van de Graaf et al., 1996).

2.4. Analytical methods

Samples from the influent and effluent were collected on a daily basis and immediately filtered through a 0.45-μm polyether sulfone membrane filter (Anpel Company, China). NH_4^+—N was measured

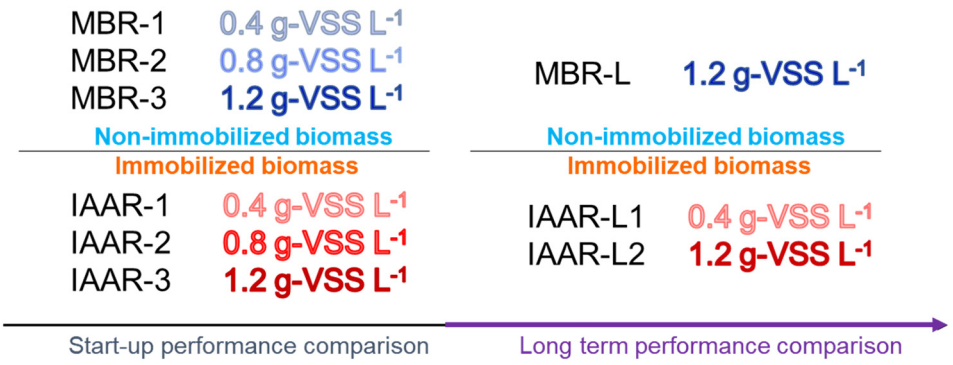

Fig. 2. Experimental design for effects of the initial biomass concentration on the performance of denitrification between IAAR (immobilized AOB and ANAMMOX bacteria reactor) and CANON-MBR.

Table 1
Conditions of long-term tests for IAARs and CANON-MBR.

Phase	Period (day)	Influent $NH_4^+ - N$ (mg L^{-1})	DO (mg L^{-1})	Nitrogen loading rate (kg-N m^{-3} d^{-1})	HRT (day)
I	1–14	61 ± 4.6	0.5 ± 0.5	0.612 ± 0.02	0.1
II	15–32	183 ± 5.1	1 ± 0.5	1.834 ± 0.04	0.1
III	33–93	410 ± 9.7	3 ± 0.5	4.083 ± 0.03	0.1

using colorimetric methods according to Standard Methods (APHA1995). NO_2^- −N and NO_3^- −N were analyzed using ion chromatography (ICS-1000, Dionex, USA) with an AS-20 column, an AG-20 guard column, and a 150 mg L^{-1} injection loop (Xia et al., 2011). Mixed liquor suspended solids (MLSS) and VSS were determined using a weight method. Nitrogen removal rate per biomass (BNRR) was calculated as the ratio of the nitrogen removal rates to the VSS of the biomass.

2.5. Microsensor analysis

Depth profiles of DO concentration were measured with an Ox-10 glass microelectrode sensor (Unisense, Denmark). The sensor tip was composed of solid glass and covered by a silicone membrane with a diameter of 10 μm. DO profiles were converted to concentration using a two-point calibration (100% and 0% O_2) (Fenchel and Glud, 2000; Thompson et al., 2003). A Unisense pH glass microelectrode was used to measure the depth profiles of the pH in the gel layers, and was connected to a high-impedance millivolt-meter (Unisense, Denmark) with a reference electrode. Specification of the electrodes and the datalogger is illustrated in detail elsewhere (Vorenhout et al., 2004). The pH electrode was calibrated in standard buffer solutions (pH = 4 and 7) before use. To measure the inner DO concentration and pH, the sensors were carefully inserted into the gel layers at a constant speed. The temperature of the solutions and layers was maintained at 35 °C throughout the microelectrode measurements.

2.6. DNA extraction and high-throughput pyrosequencing

In this study, inoculated biomass samples from the Nitritation-SBR reactor and ANAMMOX-MBR reactor from the CANON reactor were collected and stored at −80 °C for subsequent molecular processing. Genomic DNA of each sample DNA was extracted and purified using a bacterial genomic mini extraction kit (Sangon, China). The DNA was qualified using a Qubit 2.0 DNA detection kit (Sangon, China) and the qualified DNA was high-throughput pyrosequencing sequenced by the Sangon Company (Sangon, China) (Liang et al., 2015). The PCR primers were V3-V4 universe primers 341F/805R (341F: CCTACGGGNGGCWGCAG; 805R: GACTACHVGGGTATCTAATCC) (Herlemann et al., 2011; Hugerth et al., 2014). Operational taxonomic units (OTUs) were defined by clustering at 3% variation, which is assumed to correspond to the genus level. The Shannon diversity index was processed using mothur (http://www.mothur.org/), and the sequences were compared to the reference microorganisms available in the Silva database (http://www.arb-silva.de).

2.7. Fluorescence in situ hybridization

The samples harvested from the two gel layers in IAAR-L1 during phase III were fixed with 4% (w/v) paraformaldehyde in PBS (8.0 g of NaCl, 0.2 g of KCl, 1.15 g of Na_2HPO_4, KH_2PO_4, and 0.2 g L^{-1} of distilled water and a pH of 7.2) at 4 °C for 12 h (Isaka et al., 2007). Samples were washed three times with 0.5 M PBS, re-suspended in the 0.5 M PBS, and maintained at 4 °C for 3 days. To characterize the in situ microbial community structure of the AOB and ANAMMOX bacteria in the two gel layers, samples were directly cut to a mini cube using high-profile disposable microtome blades (size: 2 × 2 × 2 mm). The gel cube was covered by Teflon-coated glass slides. The ANAMMOX bacterial population in the gel layers was determined using the ROX-labeled oligonucleotide probe Amx368 (Pavlekovic et al., 2009). The AOB population in the gel layers was determined using the AMCA-labeled oligonucleotide probe NSO190. The total bacterial population in the gel layers was determined using the FAM-labeled oligonucleotide probe EUB338. (Jetten et al., 2003; Mobarry et al., 1996; Okabe et al., 1999) The hybridized samples were observed using a Nikon A1R Spectral Confocal Microscope (Nikon, Tokyo, Japan). The confocal microscope was coupled to a *Z*-stage piezo-controller. Z-series scanning was completed every 20 μm up to a Z-depth of 2000 μm using a Nikon 10 × objective lens. A three-dimensional (3D) model image of the microbial community in the two gel layers was made using the NIS–Elements AR software (4.20).

3. Results and discussion

3.1. Start-up experiments

The effects of initial biomass concentration in the six one-stage deammonification reactors were investigated and the results are shown in Fig. 3. For IAAR-1, IAAR-2, and IAAR-3, the AOB and ANAMMOX biomass was immobilized into gel layers as described in Section 2.3 with biomass concentrations of 0.4, 0.8, and 1.2 g-VSS L^{-1}, respectively For comparison, reactors MBR-1, MBR-2, and MBR-3 contained the mixed ANAMMOX and AOB aggregated biomass without immobilization and were also operated using the same initial biomass concentrations. All six reactors were operated at 35 ± 1 °C with the same nitrogen loading rate (NLR) of 0.67 kg-N m^{-3} d^{-1} for 7 days. The stoichiometric ratios of the produced nitrate to consumed ammonia in the six reactors ranged from 10% to 14%, near the 11% of the optimal deammonification process (Strous et al., 1998). As shown in Fig. 3, the nitrogen removal rate (NRR) of all the immobilized biomass reactors exceeded all the NRRs of the non-immobilized biomass reactors after 7 days of operation. IAAR-3's NRR rapidly increased from 0.04 kg-N m^{-3} d^{-1} to 0.35 kg-N m^{-3} d^{-1} during the initial 4 days, whereas for MBR-3 it slowly increased to 0.12 kg-N m^{-3} d^{-1}. The NRR of IAAR-3 reached 0.57 kg-N m^{-3} d^{-1} on the last day, which is the highest NRR among the six reactors. The NRR of MBR-1 remained at a very low level (0.07 kg-N m^{-3} d^{-1}) until the end of test, whereas the NRR of IAAR-1 increased from 0.002 kg-N m^{-3} d^{-1} to 0.502 kg-N m^{-3} d^{-1}. The final NRR of IAAR-1 with the lowest immobilized biomass concentration was still higher than that of the final NRR (0.47 kg-N m^{-3} d^{-1}) of MBR-3 with the highest non-immobilized biomass concentration. During the initial 5 days, the NRRs of the immobilized and non-immobilized biomass were in direct proportion to the initial biomass concentration: a higher initial biomass concentration resulted in a higher NRR (Fig. 3). Notably, the difference in the NRRs of all the non-immobilized reactors increased at the end of the 7-day operation. In contrast, the difference in the NRRs of the immobilized biomass reactors gradually decreased. IAAR-1, IAAR-2, and IAAR-3 containing the immobilized biomass reached the same NRR of approximately 0.5 kg-N m^{-3} d^{-1} after the 7-day operation. Fig. 3(B) shows the comparison of all the reactors' NRRs and biomass concentration unit. Under the same loading rate, the highest BNRR (nitrogen removal rate per biomass) was obtained by IAAR-1 (1.25 g-N g-VSS^{-1} d^{-1}) with the lowest biomass concentration. The BNRR of IAAR-3 (0.48 g-N g-VSS^{-1} d^{-1}) was higher than that of MBR-3 (0.38 g-N g-VSS^{-1} d^{-1}) at the end of the 7-day operation. The BNRRs of the non-immobilized biomass (MBR-1, MBR-2, and MBR-3) were in proportion to their initial biomass concentration. However, the BNRRs of the immobilized biomass (IAAR-1, IAAR-2, and IAAR-3) were inversely proportional to their respective initial biomass concentration. The short-term data of the NRRs illustrated that the performances of the IAARs were better than that of the MBRs under the same biomass concentration. Combining NRRs with BNRRs, the immobilization method used in this study can enhance the

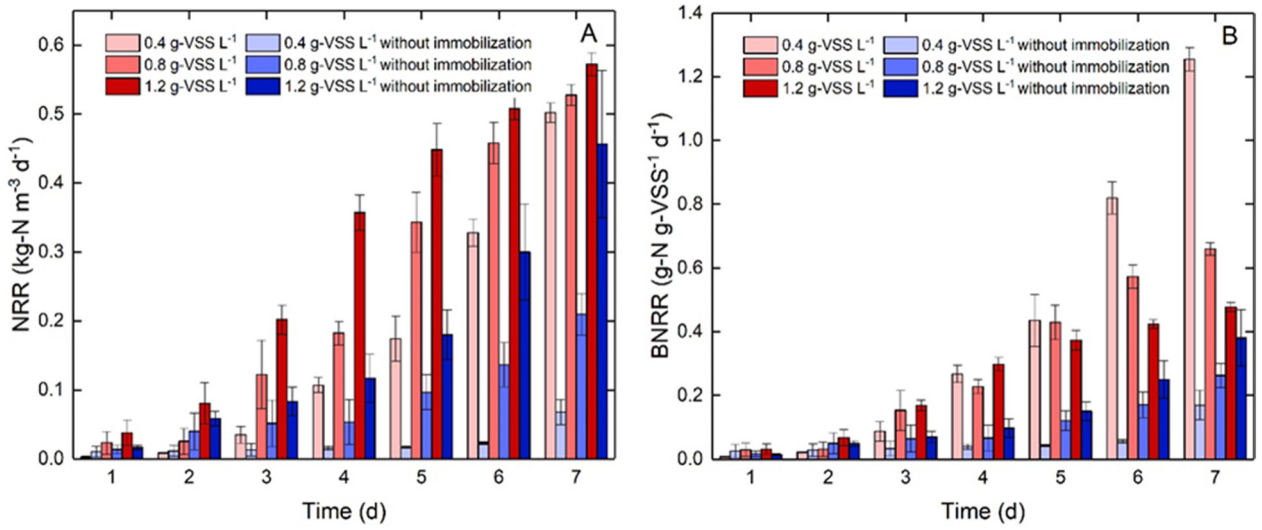

Fig. 3. Nitrogen removal rates (A) & Nitrogen removal rates per biomass (B) in six reactors containing different quantity of immobilized and non-immobilized AOB and ANAMMOX biomass under the same conditions during 7-days operation. Error bars indicate the range of standard deviations (SD) derived from triplicate measurements.

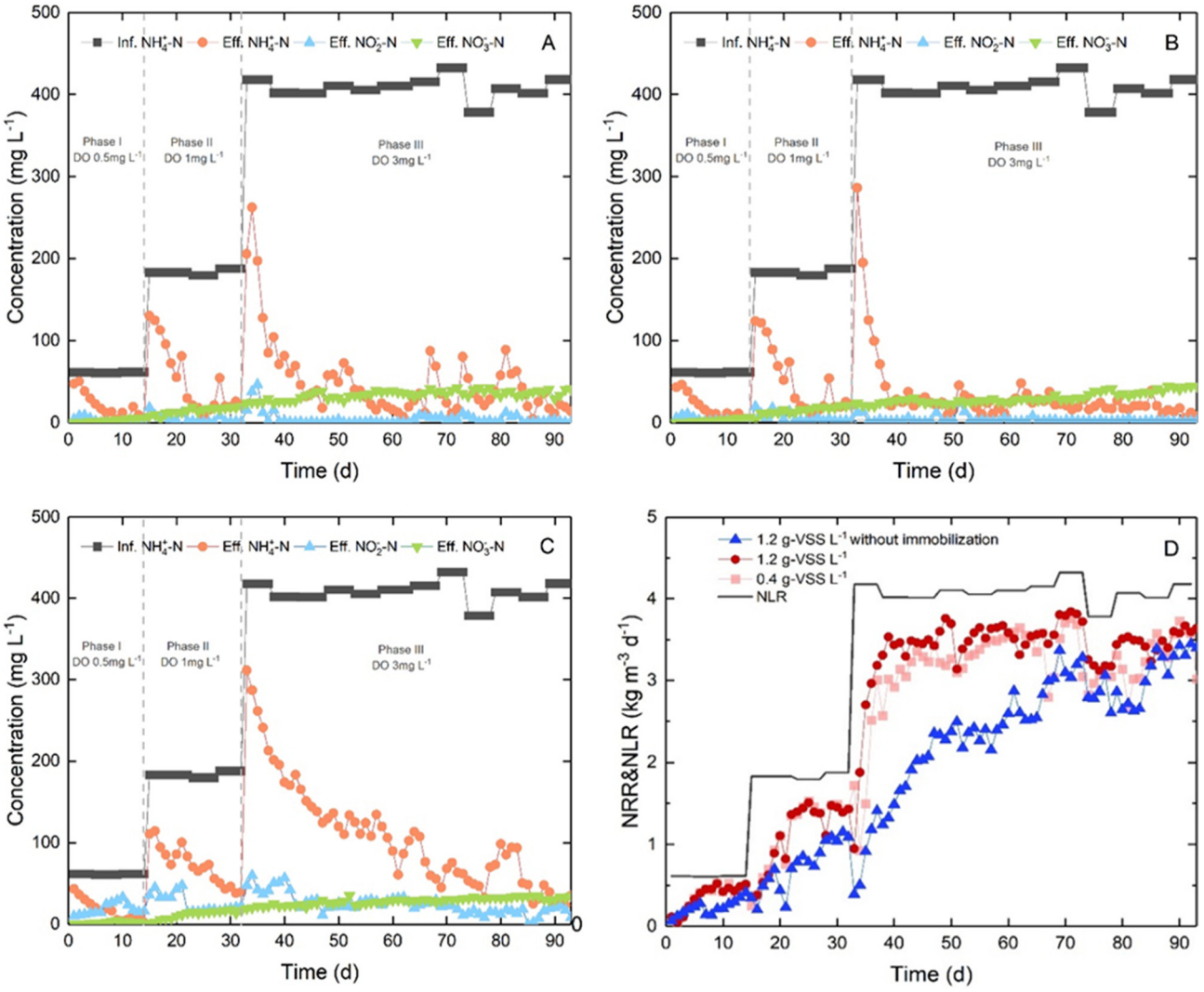

Fig. 4. Concentration of N species in IAAR-L1 (A), IAAR-L2 (B) and MBR-L (C) during about 94-days operation. Variation of NLR and NRR in three reactors (D).

activity of a low biomass concentration of AOB and ANAMMOX during the start-up period.

3.2. Long-term experiments

Continuous experiments of IAAR-L1 (0.4 g-VSS L^{-1}), IAAR-L2 (1.2 g-VSS L^{-1}), and MBR-L (1.2 g-VSS L^{-1}) were conducted for 94 days, as shown in Fig. 4. Initially, for the first 14 days, three reactors were operated with an average NLR of 0.61 kg-N m^{-3} d^{-1} under a hydraulic retention time (HRT) of 0.1 day. The DO concentration was maintained at approximately 0.5 mg L^{-1} by controlling the air flow rate during phase I. This low DO concentration (0.5 mg L^{-1}) during the start-up stage was helpful for the activation of ANAMMOX bacteria, and could reduce the possibility of nitrite inhibition. Fig. 4(A), (B) and (C) show that IAAR-L1 and IAAR-L2 had a similar nitrogen removal performance and both were better than that of MBR-L. During phases II and III, the decrease in ammonium concentration in the MBR-L effluent was obviously slower than that of IAAR-L1 and IAAR-L2. The concentration of ammonium in IAAR-L1 and IAAR-L2 was 18.4 and 9.3 mg L^{-1} on day 25, respectively, meanwhile MBR-L effluent's ammonium concentration was 69.4 mg L^{-1}. The ammonium concentration in MBR-L's effluent slowly decreased from 311.3 mg L^{-1} to 32.5 mg L^{-1} from day 33 to day 77, whereas IAAR-L1's ammonium concentration decreased to 32.1 mg L^{-1} through the first 11 days during phase III. Fig. 4(D) shows that IAAR-L1 and IAAR-L2 had a similar NRR trend during phases I and II. Based on Fig. 4(A) and (B), the effluent ammonium concentration of IAAR-L1 was not as stable as that of IAAR-L2 under a high loading rate (phase III). As the effluent ammonium concentration of IAAR-L1 suddenly increased, the NRR of IAAR-L1 decreased four times on day 51, 67, 73, and 81, respectively. The NRR of IAAR-L2 only had two small fluctuations after the increase in the loading rate. This indicated that the IAAR with a higher immobilized biomass concentration could obtain a more stable NRR under a high NLR. When the NLR and DO concentration increased at the beginning of every phase, the nitrite concentration of all three reactors increased to different levels the following days. The effluent nitrite concentration of IAAR-L2 increased from 2.6 to 13.4 mg L^{-1} and the effluent nitrite concentration of MBR-L increased from 22.5 to 59.5 mg L^{-1} during the first two days of phase III. This suggested that the adaptation time to the loading increase in the AOB biomass was shorter than that of the ANAMMOX biomass. Unlike the gradual increase in the specific activity for AOB, the ANAMMOX activity slowly increased and maximized when the influent ammonium concentration was supplied at a high level (Choi et al., 2018). The quick nitrite accumulation (greater than 50 mg L^{-1}) likely influenced the activity of the ANAMMOX bacteria, which induced the low NRR of MBR-L (Strous et al., 1999b). The nitrite concentration in IAAR-L1's and IAAR-L2's effluent was obviously lower than that of MBR-L, which means the special gel structure slowed the nitrite accumulation. However, MBR-L took 72 days to reach nearly the same NRR (3.19 kg-N m^{-3} d^{-1}) as IAAR-L2 with the same initial biomass concentration. However, IAAR-L2 reached this NRR in only 37 days. The results show that the non-immobilized bacteria in the CANON-MBR reactor required a longer time than the immobilized biomass in IAAR to adapt to a change in influent loading and DO concentration.

3.3. Comparison of start-up performances

It is interesting to compare the start-up times and removal efficiency of different one-stage deammonification reactors with our results. The criteria for a successful start-up of a one-stage autotrophic denitrification reactor in this study was defined as follows: the target NLR of the reactor is approximately 0.5 kg-N m^{-3} d^{-1} because the NLR for one of the earliest full-scale one-stage autotrophic denitrification reactors in Hattingen, Germany, was designed for approximately 0.5 kg-N m^{-3} d^{-1} (Lackner et al., 2014). Based on our experimental results, the lowest biomass concentration of 0.4 g-VSS L^{-1} (IAAR-L1) was able to meet the criteria of a successful start-up and accomplished an NRR of 0.5 kg-N m^{-3} d^{-1} in 10 days. Table 2 lists the start-up performance of different types of single-stage autotrophic nitrogen removal reactors and the start-up time to meet the NRR of 0.5 kg-N m^{-3} d^{-1} (The start-up time is the days to reach the NRR_{max} if the NRR of the reactor could not meet 0.5 kg-N m^{-3} d^{-1}) (Chen et al., 2012; Kowalski et al., 2018). Deng et al. achieved start-up in 50 days via the sequencing biofilm batch reactor with an NRR_{max} of 0.39 kg-N m^{-3} d^{-1} (Deng et al., 2016). Qiao et al. developed a moving carrier reactor (MCR) co-immobilizing 0.72 g-VSS L^{-1} partial nitrifying and ANAMMOX biomass. They started up deammonification in 58 days with an NRR_{max} of 1.69 kg-N m^{-3} d^{-1} (Qiao et al., 2013). The start-up time of the MCR developed by Isaka et al. is nearly shorter than ours (7 days after nitritation biomass started up). They used approximately 4 g-VSS L^{-1} biomass for the start-up (Isaka et al., 2013). At the same time, the NRR_{max} (1.4 kg-N m^{-3} d^{-1}) of their MCR was still lower than that of IAAR (3.73 kg-N m^{-3} d^{-1}). In comparison to many recent studies, the deammonification performances obtained by immobilized gel reactors such as the MCR and IAAR are significantly higher, approximately ten times higher, than that obtained in an SBR, MBBR, and SBBR. The MBR as a parallel reactor without immobilization in our study took more than 22 days to complete the start-up and reached 0.52 kg-N m^{-3} d^{-1}. Of particular note, the NRR_{max} and $BNRR_{max}$ of the IAAR is apparently the highest and the ANAMMOX biomass concentration (0.4 g-VSS L^{-1}) required for the start-up of the complete autotrophic nitrogen removal reactor is the lowest. Based on the comparison result, this suggests that the IAAR has the potential to reduce the amount of seed sludge for reactor start-up in a future engineering application.

3.4. In situ spatial distribution of DO and pH

The DO concentration and pH of the steady state AOB-ANAMMOX gel layers with an average thickness of 2400 ± 50 μm under the same NLR were measured using a microelectrode of a 100-μm step size (Fig. 5) during phase III. As shown in Fig. 5, the DO concentration gradually decreased from 3.0 to 0.3 mg L^{-1} between 0 μm and 1200 μm in the AOB gel layer and remained extremely low between 1200 μm and 2400 μm in the ANAMMOX gel layer. The DO concentration was less than 1 mg L^{-1} across over one-half of the AOB gel layer. After penetrating through the AOB gel layer, the DO concentration was nearly zero across the entire ANAMMOX gel layer. The nitrite transferred from the AOB part and the strict anaerobic condition in the ANAMMOX layer enabled the inside ANAMMOX bacteria to efficiently work. Fig. 5 shows

Table 2
Comparison of the performances on different types of complete autotrophic nitrogen removal reactors. MBBR: Moving bed biofilm reactors, SBR: Sequencing batch reactor, SNAP: Single-stage Nitrogen removal using ANAMMOX and Partial nitritation, MCR: Moving carrier reactor, SBBR: Sequencing Batch Biofilm Reactor.

Reactor	Carrier	Initial VSS (g-VSS L^{-1})	Start-up time (d)	NRR_{max} (kg-N m^{-3} d^{-1})	$BNNR_{max}$ (g-N $g\text{-}VSS^{-1}$ d^{-1})	Reference
SBBR	Activated carbon fibers	3	80	0.088	0.029	Chen et al. (2012)
MCR	Gel	0.72	58	1.69	2.34	Qiao et al. (2013)
SBBR	Combined packing	2.26	50	0.39	0.17	Deng et al. (2016)
MBBR	AnoxKaldnes	1.25	50	0.6	0.48	Kowalski et al., (2018)
SBR	None	6.4	35	0.51	0.08	Joss et al. (2009)
MCR	Gel	4	7	1.4	0.35	Isaka et al. (2013)
IAAR	Gel	0.4	10	3.73	9.32	Our study

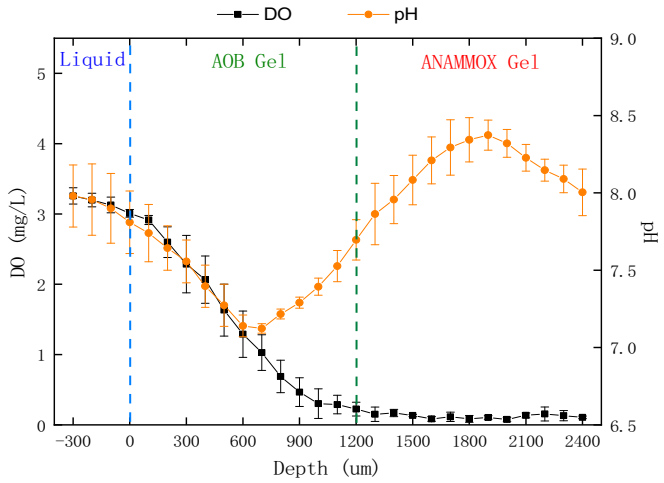

Fig. 5. Steady state concentration profiles of DO and pH in AOB-ANAMMOX gel layers at 3 mg L^{-1} in the IAAR-L1. Dashed line represents a liquid-gel interface. Error bars indicate the range of standard deviations (SD) derived from triplicate measurements.

that the pH ranged from 7.14 to 7.74 in the AOB gel layer and from 7.69 to 8.37 between 1200 and 2400 μm. Tang et al. reported that the high activity of ANAMMOX resulted in high production of acidity and the pH obviously increased. Meanwhile, Yan and Hu reported that the high activity of AOB resulted in high consumption of acidity and the pH quickly decreased (Tang et al., 2009; Yan and Hu, 2009). The great change in pH across the gel layers corresponded to the high NRR_{avg} (the average NRR) of 3.17 kg-N m^{-3} d^{-1} during phase III, illustrating the high activity of the nitritation and ANAMMOX reactions in the gel layers. The microsensor data shown in Fig. 5 suggests that 3 mg L^{-1} of liquid DO concentration below the AOB gel layer was the most appropriate amount for the IAAR-L1 with a 0.4 g-VSS L^{-1} biomass concentration. The low DO concentration in the AOB part could not ensure the normal reaction of ammonium oxidization, which may explain the low nitritation rate and poor ANAMMOX performance. According to Liu et al., when the size of aerobic granules is greater than 0.5 mm, DO becomes a major limiting factor of metabolic activity of AOB over a substrate (Liu et al., 2012). Vlaeminck et al. showed that the activity and abundance of ANAMMOX bacteria is directly proportional to the size of the granules and the activity and abundance of AOB is inversely proportional (Vlaeminck et al., 2010). At the same time, a high DO concentration would cause a high nitrite accumulation and nitrite inhibition of ANAMMOX biomass (Qiao et al., 2013; Vlaeminck et al., 2010). As we can see in Fig. 4(C), the CANON-MBR with non-immobilized biomass could result in problems of the nitrite accumulation and low NRR every time the NLR and DO level increased.

3.5. In situ FISH analysis

To explain the spatial distribution of the AOB and ANAMMOX bacteria during the steady state of phase III, AOB-ANAMMOX gel layers from IAAR-L1 were analyzed using FISH analysis on day 80 under a Nikon A1R Spectral, as shown in Fig. 6. FISH was performed using a FAM-labeled probe EUB338 (blue) for most members of Eubacteria. FISH results showed large amounts of ANAMMOX bacteria (red) in the upper layer of the gel cube, whereas more AOB distribution (green) was detected in the lower layer of the gel cube. These results are, to the authors' knowledge, the first reported 3D reconstruction of a model of an in situ microbial community in two gel layers via confocal microscopy.

As shown in Figs. 5 and 6, the DO spatial distribution and FISH images demonstrate that the spatial structure of the gel layers established for the AOB and ANAMMOX biomasses were excellent and could mediate the DO requirement between nitritation and the ANAMMOX process in a single-stage reactor. As shown in Fig. 6, the AOB and ANAMMOX bacteria were evenly distributed within their respective layers. Compared to natural PN/A process biofilms or aggregates, immobilization technology could enable biomass to be more effectively organized and to be more efficiently fed in the gel. During phase III, FISH analysis shows the AOB existed in the gel between 0 μm and 1200 μm, where the DO concentration ranged from 3.0 to 0.3 mg L^{-1}. At the same time, the FISH analysis image shows the ANAMMOX bacteria existed in the gel between 1200 μm and 2400 μm, where the DO concentration ranged from 0.1 to 1 mg L^{-1}. Therefore, the appropriate growth conditions of the two bacteria resulted in IAAR-L1 reaching a high NRR (0.76 kg m^{-3} d^{-1}). Biofilms or aggregates formed in CANON, DEMON®, or SNAP (single-stage nitrogen removal using ANAMMOX and partial nitritation processes) systems are based on the hypothesis that the nitritation reaction occurs in the outer portions of the aggregate under oxygen-supplied conditions and the ANAMMOX reaction occurs in the inner portions under oxygen-limited conditions (Gonzalez-Martinez et al., 2016; Nielsen et al., 2005; Third et al., 2001). Forming an adequate natural biofilm or aggregate with an outside layer and an inside layer would be prohibitively time-consuming. In contrast, our research constructed a good gel structure for two types of bacteria using a few simple steps. Thus, the start-up time (10 days) for deammonification in our reactor is shorter than many other reported processes.

Biomass density and distribution are also important factors in biomass substrate transmission. Because the biomass density and diffusion ability of substrates in naturally formed granular were uncontrollable, it was difficult to mediate the different growth environments between AOB and ANAMMOX biomass. The low biomass density of AOB in the out layer could cause a shortage of nitrite and accumulation of DO in the inner layer. High biomass density and ineffective diffusion of substrates prevented interior ANAMMOX biomass from receiving the nitrite and removing nitrogen in the large granular (Furukawa et al., 2006; Joss et al., 2009; Sliekers et al., 2003). The effective diffusion coefficients of NH_4^+—N at 37 °C in the granular and immobilized biomass with SA gel were determined to be $8.6 \pm 2.3 \times 10^{-6}$ cm^2 s^{-1} and $29.0 \pm 6.7 \times 10^{-6}$ cm^2 s^{-1}, respectively (Ali et al., 2015). The higher diffusivity and homogeneous distribution consequently led to a positive environment for the retained AOB and ANAMMOX bacterial metabolism in our study, resulting in a higher NRR_{max} (3.73 kg-N m^{-3} d^{-1}) than that of the granular biomass even at an IAAR biomass concentration of 0.4 g-VSS L^{-1}.

4. Conclusions

An IAAR was developed for a one-stage deammonification process. Although the IAAR could be easily established using a low quantity of biomass, the nitrogen removal performance was excellent. The start-up performances demonstrated that the BNRR of IAAR-1 with a 0.4 g-VSS L^{-1} biomass concentration reached 1.25 g-N g-VSS^{-1} d^{-1} in 7 days, and the CANON-MBR with a 1.2 g-VSS L^{-1} biomass concentration only reached 0.38 g-N g-VSS^{-1} d^{-1}. IAAR-L1 (0.4 g-VSS L^{-1}) started up quickly in 10 days and achieved an NRR_{max} of 3.73 kg-N m^{-3} d^{-1}. The CANON-MBR with non-immobilized biomass took 22 days to finish the start-up and required a longer time adapting to the increase in NLR and DO concentration compared to that of the IAAR. In situ microelectrode measurement inside the AOB-ANAMMOX gel layers proved that the double gel layer structure had an ideal permeation profile of DO concentration and pH under an NLR of approximately 4.0 kg-N m^{-3} d^{-1}. Excellent spatial distributions of AOB and ANAMMOX bacteria were proven in situ by FISH analysis, which matched the results of the DO distribution. These results indicate that an IAAR is among the most effective reactor configurations for quick start-up and stable operation of the deammonification process using a small quantity of initial biomass (0.4 g-VSS L^{-1}).

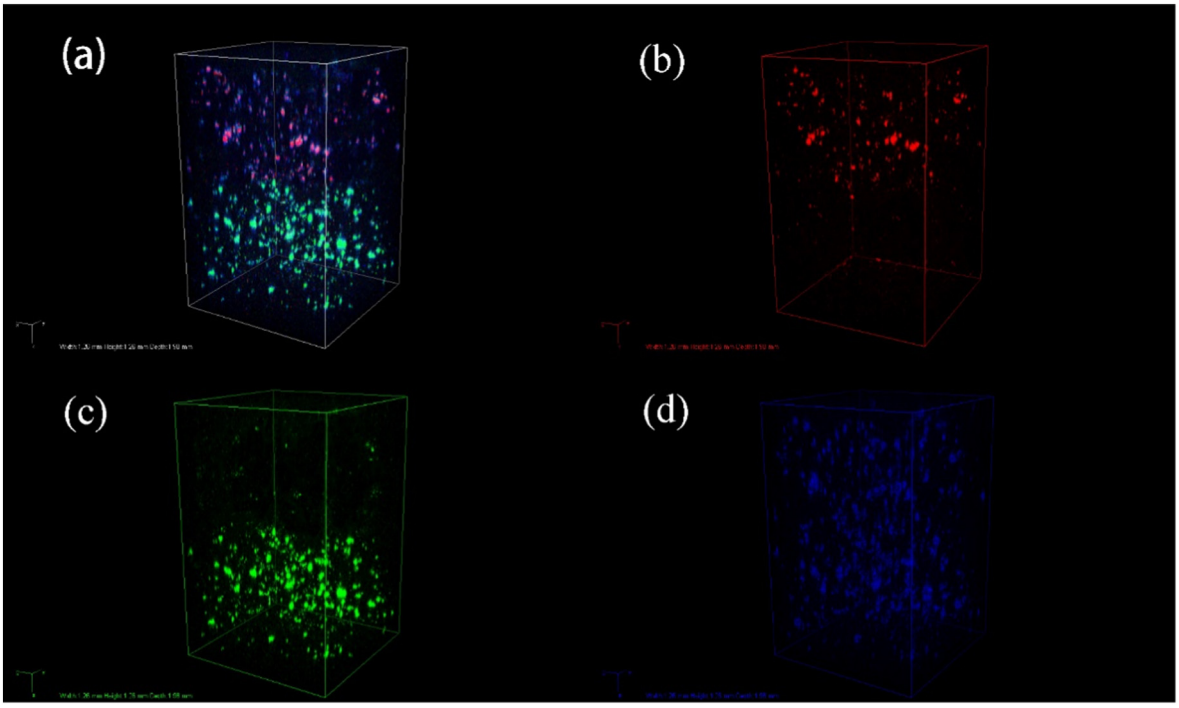

Fig. 6. Confocal laser scanning microscope images of cross-section of in situ AOB-ANAMMOX immobilization gel layers on the day 80, showing the microbial community with a FAM-labeled probe EUB338 of most members of Eubacteria (blue color; 6(d)), a ROX-labeled probe of ANAMMOX bacteria (red color; 6(b)), and an AMCA-labeled probe NSO190 of AOB bacteria (green color, 6(c)), and an overlay of all these probes (6(a)). Both probes EUB338 and NSO190 hybridized with AOB, resulting in cyan signal. Both probes EUB338 and Amx820 hybridized with ANAMMOX, resulting in a purple-red signal. (For interpretation of the references to color in this figure legend, the reader is referred to the web version of this article.)

Acknowledgements

This work was supported by National Key Research and Development program of China [2017YFC0403403], and the Foundation of State Key Laboratory of Pollution Control and Resource Reuse (Tongji University) [PCRRT16003].

Appendix A. Supplementary data

Supplementary data to this article can be found online at https://doi.org/10.1016/j.scitotenv.2018.11.069.

References

Ali, M., Oshiki, M., Rathnayake, L., Ishii, S., Satoh, H., Okabe, S., 2015. Rapid and successful start-up of anammox process by immobilizing the minimal quantity of biomass in PVA-SA gel beads. Water Res. 79, 147–157.

Cai, M.-Q., Hu, J.-Q., Wells, G., Seo, Y., Spinney, R., Ho, S.-H., et al., 2018. Understanding mechanisms of synergy between acidification and ultrasound treatments for activated sludge dewatering: from bench to pilot–scale investigation. Environ. Sci. Technol. 52, 4313–4323.

Chen, Y.P., Li, S., Ning, Y.F., Hu, N.N., Cao, H.H., Fang, F., et al., 2012. Start-up of completely autotrophic nitrogen removal over nitrite enhanced by hydrophilic-modified carbon fiber. Appl. Biochem. Biotechnol. 166, 866–877.

Choi, D., Cho, S., Jung, J., 2018. Key operating parameters affecting nitrogen removal rate in single-stage deammonification. Chemosphere 207, 357–364.

Corbalá-Robles, L., Picioreanu, C., van Loosdrecht, M.C., Pérez, J., 2016. Analysing the effects of the aeration pattern and residual ammonium concentration in a partial nitritation-anammox process. Environ. Technol. 37, 694–702.

Deng, Y., Zhang, X., Miao, Y., Hu, B., 2016. Exploration of rapid start-up of the CANON process from activated sludge inoculum in a sequencing biofilm batch reactor (SBBR). Water Sci. Technol. 73, 535–542.

Egli, K., Fanger, U., Alvarez, P.J., Siegrist, H., van der Meer, J.R., Zehnder, A.J., 2001. Enrichment and characterization of an anammox bacterium from a rotating biological contactor treating ammonium-rich leachate. Arch. Microbiol. 175, 198–207.

Fenchel, T., Glud, R.N., 2000. Benthic primary production and O_2-CO_2 dynamics in a shallow-water sediment: spatial and temporal heterogeneity. Ophelia 53, 159–171.

Furukawa, K., Lieu, P., Tokitoh, H., Fujii, T., 2006. Development of single-stage nitrogen removal using anammox and partial nitritation (SNAP) and its treatment performances. Water Sci. Technol. 53, 83–90.

Gonzalez-Martinez, A., Rodriguez-Sanchez, A., Garcia-Ruiz, M.J., Muñoz-Palazon, B., Cortes-Lorenzo, C., Osorio, F., et al., 2016. Performance and bacterial community dynamics of a CANON bioreactor acclimated from high to low operational temperatures. Chem. Eng. J. 287, 557–567.

Herlemann, D.P., Labrenz, M., Jürgens, K., Bertilsson, S., Waniek, J.J., Andersson, A.F., 2011. Transitions in bacterial communities along the 2000 km salinity gradient of the Baltic Sea. The ISME Journal 5, 1571–1579.

Hugerth, L.W., Wefer, H.A., Lundin, S., Jakobsson, H.E., Lindberg, M., Rodin, S., et al., 2014. DegePrime, a program for degenerate primer design for broad-taxonomic-range pcr in microbial ecology studies. Appl. Environ. Microbiol. 80, 5116–5123.

Isaka, K., Date, Y., Kimura, Y., Sumino, T., Tsuneda, S., 2008. Nitrogen removal performance using anaerobic ammonium oxidation at low temperatures. FEMS Microbiol. Lett. 282, 32–38.

Isaka, K., Date, Y., Sumino, T., Tsuneda, S., 2007. Ammonium removal performance of anaerobic ammonium-oxidizing bacteria immobilized in polyethylene glycol gel carrier. Appl. Microbiol. Biotechnol. 76, 1457–1465.

Isaka, K., Kimura, Y., Yamamoto, T., Osaka, T., Tsuneda, S., 2013. Complete autotrophic denitrification in a single reactor using nitritation and anammox gel carriers. Bioresour. Technol. 147, 96–101.

Jetten, M.S., Sliekers, O., Kuypers, M., Dalsgaard, T., van Niftrik, L., Cirpus, I., et al., 2003. Anaerobic ammonium oxidation by marine and freshwater planctomycete-like bacteria. Appl. Microbiol. Biotechnol. 63, 107–114.

Jetten, M.S.M., Strous, M., van de Pas-Schoonen, K.T., Schalk, J., van Dongen, U.G.J.M., van de Graaf, A.A., et al., 1998. The anaerobic oxidation of ammonium. FEMS Microbiol. Rev. 22, 421–437.

Joss, A., Salzgeber, D., Eugster, J., König, R., Rottermann, K., Burger, S., et al., 2009. Full-scale nitrogen removal from digester liquid with partial nitritation and anammox in one SBR. Environ. Sci. Technol. 43, 5301–5306.

Kowalski, M.S., Devlin, T.R., Oleszkiewicz, J.A., 2018. Start-up and long-term performance of anammox moving bed biofilm reactor seeded with granular biomass. Chemosphere 200, 481–486.

Lackner, S., Gilbert, E.M., Vlaeminck, S.E., Joss, A., Horn, H., van Loosdrecht, M.C., 2014. Full-scale partial nitritation/anammox experiences–an application survey. Water Res. 55, 292–303.

Liang, Y., Li, D., Zhang, X., Zeng, H., Yang, Y., Zhang, J., 2015. Nitrate removal by organotrophic anaerobic ammonium oxidizing bacteria with C_2/C_3 fatty acid in upflow anaerobic sludge blanket reactors. Bioresour. Technol. 193, 408–414.

Liu, T., Li, D., Zeng, H., Li, X., Zeng, T., Chang, X., et al., 2012. Biodiversity and quantification of functional bacteria in completely autotrophic nitrogen-removal over nitrite (CANON) process. Bioresour. Technol. 118, 399–406.

Luo, S., Gao, L., Wei, Z., Spinney, R., Dionysiou, D.D., Hu, W.-P., et al., 2018. Kinetic and mechanistic aspects of hydroxyl radical–mediated degradation of naproxen and reaction intermediates. Water Res. 137, 233–241.
Lv, Y., Ju, K., Wang, L., Sun, T., Miao, R., Wang, X., et al., 2016. In situ probing of microbial activity within anammox granular biomass with microelectrodes. J. Biosci. Bioeng. 121, 450–456.
Min, X., Li, W., Wei, Z., Spinney, R., Dionysiou, D.D., Seo, Y., et al., 2018. Sorption and biodegradation of pharmaceuticals in aerobic activated sludge system: a combined experimental and theoretical mechanistic study. Chem. Eng. J. 342, 211–219.
Mobarry, B.K., Wagner, M., Urbain, V., Rittmann, B.E., Stahl, D.A., 1996. Phylogenetic probes for analyzing abundance and spatial organization of nitrifying bacteria. Appl. Environ. Microbiol. 62, 2156–2162.
Morales, N., Val Del Rio, A., Vazquez-Padin, J.R., Gutierrez, R., Fernandez-Gonzalez, R., Icaran, P., et al., 2015. Influence of dissolved oxygen concentration on the start-up of the anammox-based process: ELAN(R). Water Sci. Technol. 72, 520–527.
Nielsen, M., Bollmann, A., Sliekers, O., Jetten, M., Schmid, M., Strous, M., et al., 2005. Kinetics, diffusional limitation and microscale distribution of chemistry and organisms in a CANON reactor. FEMS Microbiol. Ecol. 51, 247–256.
Okabe, S., Satoh, H., Watanabe, Y., 1999. In situ analysis of nitrifying biofilms as determined by in situ hybridization and the use of microelectrodes. Appl. Environ. Microbiol. 65, 3182–3191.
Pavlekovic, M., Schmid, M.C., Schmider-Poignee, N., Spring, S., Pilhofer, M., Gaul, T., et al., 2009. Optimization of three FISH procedures for in situ detection of anaerobic ammonium oxidizing bacteria in biological wastewater treatment. J. Microbiol. Methods 78, 119–126.
Qiao, S., Tian, T., Duan, X., Zhou, J., Cheng, Y., 2013. Novel single-stage autotrophic nitrogen removal via co-immobilizing partial nitrifying and anammox biomass. Chem. Eng. J. 230, 19–26.
Sliekers, A.O., Third, K., Abma, W., Kuenen, J., Jetten, M., 2003. CANON and anammox in a gas-lift reactor. FEMS Microbiol. Lett. 218, 339–344.
Strous, M., Fuerst, J.A., Kramer, E.H., Logemann, S., Muyzer, G., van de Pas-Schoonen, K.T., et al., 1999b. Missing lithotroph identified as new planctomycete. Nature 400, 446–449.
Strous, M., Heijnen, J., Kuenen, J., Jetten, M., 1998. The sequencing batch reactor as a powerful tool for the study of slowly growing anaerobic ammonium-oxidizing microorganisms. Appl. Microbiol. Biotechnol. 50, 589–596.
Strous, M., Kuenen, J.G., Jetten, M.S., 1999a. Key physiology of anaerobic ammonium oxidation. Appl. Environ. Microbiol. 65, 3248–3250.
Strous, M., Van Gerven, E., Zheng, P., Kuenen, J.G., Jetten, M.S., 1997. Ammonium removal from concentrated waste streams with the anaerobic ammonium oxidation (anammox) process in different reactor configurations. Water Res. 31, 1955–1962.
Tang, C.-J., Zheng, P., Mahmood, Q., J-W, Chen, 2009. Start-up and inhibition analysis of the anammox process seeded with anaerobic granular sludge. J. Ind. Microbiol. Biotechnol. 36, 1093.
Third, K., Sliekers, A.O., Kuenen, J., Jetten, M., 2001. The CANON system (completely autotrophic nitrogen-removal over nitrite) under ammonium limitation: interaction and competition between three groups of bacteria. Syst. Appl. Microbiol. 24, 588–596.
Thompson, J.K., Peterson, M.R., Freeman, R.D., 2003. Single-neuron activity and tissue oxygenation in the cerebral cortex. Science 299, 1070–1072.
Tokutomi, T., Yamauchi, H., Nishimura, S., Yoda, M., Abma, W., 2011. Application of the nitritation and anammox process into inorganic nitrogenous wastewater from semiconductor factory. J. Environ. Eng. 137, 146–154.
van de Graaf, A.A., de Bruijn, P., Robertson, L.A., Jetten, M.S., Kuenen, J.G., 1996. Autotrophic growth of anaerobic ammonium-oxidizing micro-organisms in a fluidized bed reactor. Microbiology 142, 2187–2196.
Van Kempen, R., Mulder, J., Uijterlinde, C., Loosdrecht, M., 2001. Overview: full scale experience of the SHARON® process for treatment of rejection water of digested sludge dewatering. Water Sci. Technol. 44, 145–152.
Varas, R., Guzmán-Fierro, V., Giustinianovich, E., Behar, J., Fernández, K., Roeckel, M., 2015. Startup and oxygen concentration effects in a continuous granular mixed flow autotrophic nitrogen removal reactor. Bioresour. Technol. 190, 345–351.
Vlaeminck, S.E., Terada, A., Smets, B.F., De Clippeleir, H., Schaubroeck, T., Bolca, S., et al., 2010. Aggregate size and architecture determine microbial activity balance for one-stage partial nitritation and anammox. Appl. Environ. Microbiol. 76, 900–909.
Vorenhout, M., van der Geest, H.G., van Marum, D., Wattel, K., Eijsackers, H.J., 2004. Automated and continuous redox potential measurements in soil. J. Environ. Qual. 33, 1562–1567.
Xia, S., Li, H., Zhang, Z., Zhang, Y., Yang, X., Jia, R., et al., 2011. Bioreduction of parachloronitrobenzene in drinking water using a continuous stirred hydrogen-based hollow fiber membrane biofilm reactor. J. Hazard. Mater. 192, 593–598.
Xiao, R., Luo, Z., Wei, Z., Luo, S., Spinney, R., Yang, W., et al., 2018. Activation of peroxymonosulfate/persulfate by nanomaterials for sulfate radical-based advanced oxidation technologies. Curr. Opin. Chem. Eng. 19, 51–58.
Xu, G., Zhou, Y., Yang, Q., Lee, Z.M.-P., Gu, J., Lay, W., et al., 2015. The challenges of mainstream deammonification process for municipal used water treatment. Appl. Microbiol. Biotechnol. 99, 2485–2490.
Yan, J., Hu, Y., 2009. Partial nitrification to nitrite for treating ammonium-rich organic wastewater by immobilized biomass system. Bioresour. Technol. 100, 2341–2347.
Yang, Z., Su, R., Luo, S., Spinney, R., Cai, M., Xiao, R., et al., 2017. Comparison of the reactivity of ibuprofen with sulfate and hydroxyl radicals: an experimental and theoretical study. Sci. Total Environ. 590-591, 751–760.
Zhu, G.L., Yan, J., Hu, Y.Y., 2014. Anaerobic ammonium oxidation in polyvinyl alcohol and sodium alginate immobilized biomass system: a potential tool to maintain anammox biomass in application. Water Sci. Technol. 69, 718–726.